Polymer 49 (2008) 4989–4994

Contents lists available at ScienceDirect

Polymer

journal homepage: www.elsevier.com/locate/polymer

Poly(L-lactide) brushes on magnetic multiwalled carbon nanotubes by in-situ ring-opening polymerization

Jiangtao Feng, Wei Cai*, Jiehe Sui, Zhiguo Li, Jiaqi Wan, Ali Nabipour Chakoli

School of Material Science and Engineering, P.O. Box 405, Harbin Institute of Technology, Harbin 150001, Heilongjiang Province, PR China

ARTICLE INFO

Article history:
Received 1 March 2008
Received in revised form 18 July 2008
Accepted 6 September 2008
Available online 27 September 2008

Keywords:
Magnetic carbon nanotubes
Poly(L-lactide)
Superparamagnetism

ABSTRACT

Biodegradable poly(L-lactide) (PLLA) has been covalently grafted onto the surface of magnetic multi-walled carbon nanotubes (*m*-MWCNTs) by in-situ ring-opening polymerization of lactide. The content of grafting PLLA can be controlled by adjusting the feed ratio of monomer to *m*-MWCNTs. FT-IR and Raman spectroscopy confirm that PLLA have been covalently attached to the sidewalls of *m*-MWCNTs. Thermal gravimetric analysis (TGA) indicates that the composites of PLLA grafted *m*-MWCNTs have a polymer weight percentage of ca. 25.6–33.7 wt%. The scanning eletron microscopy (SEM) and transmission electron microscopy (TEM) are utilized to image the PLLA grafted *m*-MWCNTs, showing relatively uniform polymer layer coated on the surface of *m*-MWCNTs. The composites of PLLA grafted *m*-MWCNTs exhibit superparamagnetic behavior at room temperature and are aligned under a low magnetic field.

1. Introduction

Since their discovery in 1991[1], carbon nanotubes (CNTs) have generated huge activity in most areas of science and engineering due to their unprecedented thermal conductivity, electrical and mechanical properties [2]. It is believed that the addition of CNTs into polymers could improve the performance of many CNTs–polymer composites and open up new applications [3–5].

Poly(L-lactide) (PLLA) is linear aliphatic thermoplastic polyester, which has good thermal plasticity, shape memory property, biodegradabililty and biocompatibility. PLLA has been widely used in tissue engineering, drug delivery system and implant materials [6–8]. However, the mechanical properties of PLLA for high load bearing biomedical applications are insufficient [8]. To overcome the drawback, many approaches were carried out to improve the mechanical properties of PLLA. Biphasic calcium phosphate (BCP) was used as reinforcement to increase the mechanical properties of PLLA [9]. Zhang et al.[10] prepared PLLA/bioglass composites by phase separation of polymer solutions, and the elastic modulus of composites increased with the increase of glass content. Chen et al. [11–13] reported that PLLA functionalized CNTs by reacting functional group COCl on the surface of CNTs or using the surface initiating ring-open polymerization of L-lactide. And then, the tensile modulus and strength of PLLA were increased while the PLLA functionalized CNTs as reinforcement were incorporated to the PLLA matrix. Although the strong interfacial bonding and proper dispersion of the fillers in the polymer by in-situ polymerization could improve the mechanical properties, it is better to enhance the mechanical properties when the fillers can be aligned in the polymer matrix. Kimura et al. [14] have succeeded to align carbon nanotubes in the polystyrene matrix under a constant magnetic field of 10 T. Kordàs et al. [15] demonstrated an efficient alignment of carboxyl functionalized CNTs that had remanent iron catalyst particles in aqueous solutions under magnetic fields of 1017 mT.

For the above purpose, the magnetic-CNTs (*m*-CNTs) have been synthesized in the previous report [16] for the alignment in the polymer matrix under the low uniform magnetic field. In this present research, for the strong interfacial bonding, the composites of PLLA grafted *m*-CNTs (*m*-CNTs-*g*-PLLA) have been synthesized by "grafting from" technique. The grafting from technique refers to forming possibly dense polymer brushes via in-situ polymerization of monomers initiated by the initiating sites on the CNTs' surface [12]. The composites of *m*-CNTs-*g*-PLLA

Table 1
Reaction conditions and results for grafting PLLA from *m*-MWCNTs surfaces

Sample	R_{wt}[a]	Polymer [wt%]	M_n[b]	M_w/M_n
m-MWCNTs-*g*-PLLA-1	14/0.066	33.7	14,185	1.17
m-MWCNTs-*g*-PLLA-2	7/0.066	29.3	23,397	1.18
m-MWCNTs-*g*-PLLA-3	3/0.066	25.6	12,059	1.19

[a] Weight feed ratio of L-lactide/*m*-MWCNTs; for PLLA, R_{wt} is the weight of L-lactide.
[b] The number-average molecular weights of free polymer.

* Corresponding author. Tel.: +86 451 86418649; fax: +86 451 86415083.
E-mail address: weicai@hit.edu.cn (W. Cai).

0032-3861/$ – see front matter Crown Copyright © 2008 Published by Elsevier Ltd. All rights reserved.
doi:10.1016/j.polymer.2008.09.022

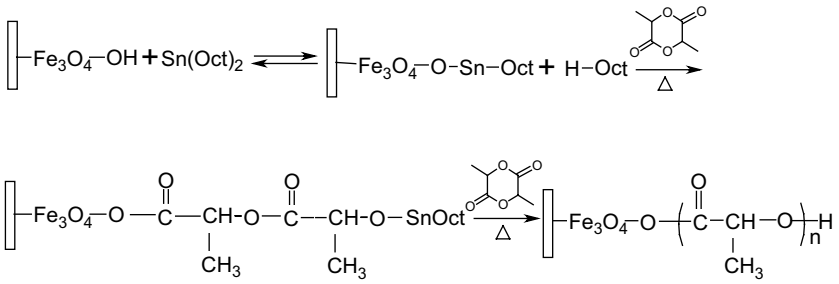

Fig. 1. Illustration for the PLLA grafting from the sidewall of *m*-MWCNTs.

are so attractive for the following reasons: 1) The interaction between the *m*-CNTs and polymers matix will become stronger because of brushed PLLA on the surface of *m*-CNTs. 2) *m*-CNTs-*g*-PLLA can be aligned orientedly and easily in the polymer matrix in the low magnetic field, although the pristine CNTs could be aligned in high magnetic field [14,15]. 3) *m*-CNTs-*g*-PLLA possess superior mechanical, electronic, superparamagnetic and biocompatible properties, which means that *m*-CNTs-*g*-PLLA will have great potential applications in the fields of nanobiomaterials and nanotechnology, and the addition of *m*-CNTs-*g*-PLLA can endue novel properties to PLLA and other biodegradable polymers. In this paper, the composites of *m*-CNTs-*g*-PLLA are characterized by thermal gravimetric analysis (TGA), Fourier transform infrared (FT-IR) spectroscopy, Raman spectroscopy, scanning electron microscopy (SEM) and magnetic property measurement system (MPMS).

2. Experimental

2.1. Materials

Multiwalled carbon nanotubes (MWCNTs) were purchased from the Nanotech Port company, Shenzhen, China (the diameter is 30–60 nm, the length is 5–15 μm, special surface area is 40–300 m^2/g). Iron(iii) acetylacetonate ($Fe(acac)_3$, 99%) was purchased from Acros. Triethylene glycol (TREG, 99%) was from Aldrich. High purity water (18.2 MΩ cm^{-1}) was obtained from a GenPure ultrapure water 105 system (TKA, Germany). L-Lactic acid (PURAC Biochem Spain.) was used as received. $Sn(Oct)_2$ (Shanghai chemical reagent company, China) was used as an initiator. All other reagents of analytical grade were used as received.

2.2. Preparation of PLLA grafted m-MWCNTs

The synthesis of the *m*-MWCNTs has been reported previously [16]. A typical procedure for *m*-MWCNTs surface grafting is described as follows: the prepared lactide (7 g) and *m*-MWCNTs (0.066 g) were placed into a flask. 0.006 mol $Sn(Oct)_2$ was injected into the flask using a syringe. Then, the flask was sealed under vacuum and heated in an oil bath at 130 °C for 48 h. The resulted product was dissolved in chloroform and subsequently separated from chloroform using a magnet. The separated product was redispersed in chloroform and washed, again. To remove the ungrafted PLLA completely, the cycle of dispersing, washing and separating was repeated at least five times. The final product was collected by a magnet and dried at 60 °C for 12 h. The free polymer were collected by precipitating in an excess of methanol and dried in a vacuum oven at 60 °C for 24 h to remove the residual solvent.

2.3. Characterization of m-MWCNTs-g-PLLA

The molecular weights were measured by WATERS 410 gel permeation chromatography (GPC) with polystyrene as column standard and using tetrahydrofuran (THF) as solvent. FT-IR spectra were recorded on a Perkin Elmer Spectrum One in the 450–4000 cm^{-1} region using KBr pellets. The Raman spectra were obtained in 400–4000 cm^{-1} region using a HORIBA Jobin Yvon HR 800 Raman spectrophotometer with 532 nm radiation from an Ar ion laser excitation source. TGA was carried out on a simultaneous

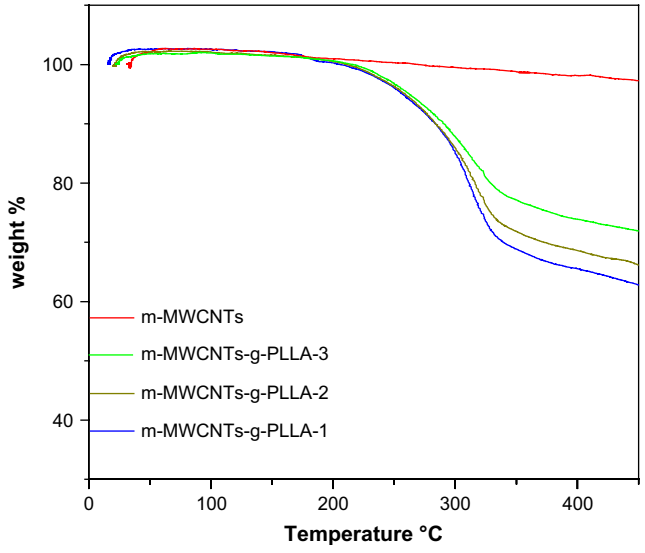

Fig. 2. TGA traces of *m*-MWCNTs and *m*-MWCNTs-*g*-PLLA.

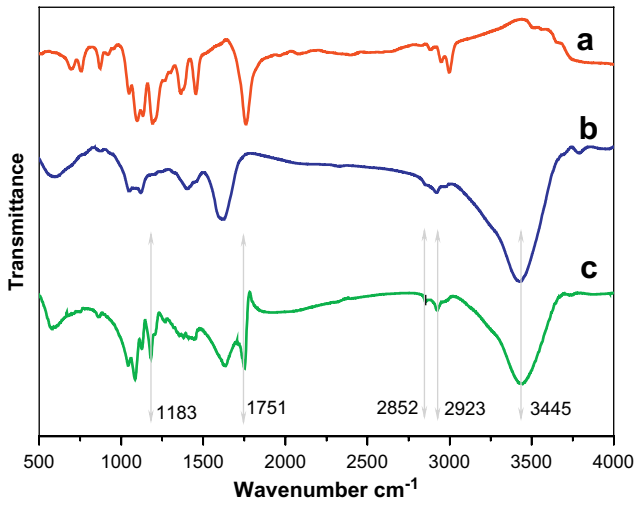

Fig. 3. FT-IR spectra of (a) PLLA, (b) *m*-MWCNTs and (c) *m*-MWCNTs-*g*-PLLA.

thermal analyzer (ZRY-2P) with a heating rate of 20 °C min^{-1} in a nitrogen flow (20 ml min^{-1}). SEM images were obtained on a Hitachi S-4700 field-emission system. TEM analysis was performed on a FEI TECANAIG^2 electron microscope at 200 kV. The magnetic property was characterized by Quantum Design MPMS XL5 SQUID magnetometer with a magnetic field ranging from −5 to 5 T.

3. Results and discussion

PLLA is grafted from the surface of *m*-MWCNTs by the ring-opening polymerization of lactide monomers. The reaction conditions and results are shown in Table 1. The polymerization is initiated by $Sn(Oct)_2$ together with hydroxyl group on the surface of *m*-MWCNTs [16]. $Sn(Oct)_2$ is considered as the low risk of racemization, high efficiency, and relatively low toxicity [17]. Recent mechanistic studies [18,19] have manifested that $Sn(Oct)_2$, in the pristine state, does not contain any reactive alkoxide groups. As the hydroxyl group is employed as coinitiator, it usually substitutes at least one of the octanoate groups of $Sn(Oct)_2$, and the resulting Sn alkoxide is then the true initiator of the polymerization process (Fig. 1).

For estimating the molar mass of grafted polymer, the molecular weights of free polymers are measured by GPC and the results are listed in Table 1. The grafting rate of PLLA is analyzed by TGA. As shown in Fig. 2, the weight loss of the *m*-MWCNTs-*g*-PLLA takes place near 300 °C due to the degradation of PLLA grafted to the *m*-MWCNTs. The amount of PLLA bound to the *m*-MWCNTs ranges from 25.6 to 33.7 wt% as the weight feed ratio (R_{wt}) rises from 3:0.066 to 14:0.066 (Table 1). Therefore, the grafted polymer content can be roughly controlled by adjusting the feed ratio.

Table 2
Raman resonances of the *m*-MWCNTs and *m*-MWCNTs-*g*-PLLA composites

Samples	FWHM(D)	FWHM(G)	Relative intensity ($I_G/I_{D'}$)	Relative intensity ($I_D/I_{D'}$)
m-MWCNTs	53.46	69.7	1.83	2.09
m-MWCNTs-*g*-PLLA-1	62.56	51	1.96	2.7
m-MWCNTs-*g*-PLLA-2	59.03	53	1.98	2.17
m-MWCNTs-*g*-PLLA-3	57.29	53	2.2	3.02

The composition of the resulting *m*-MWCNTs-*g*-PLLA is confirmed by FT-IR. Fig. 3 shows the FT-IR spectra of PLLA, *m*-MWCNTs and *m*-MWCNTs-*g*-PLLA. In Fig. 3c, a strong carbonyl stretching band at 1751 cm^{-1} reveals the ester bonds that come from the PLLA grafted to the *m*-MWCNTs. The peaks at 2923 and 1183 cm^{-1} are assigned to C–H stretching vibration and the C–O

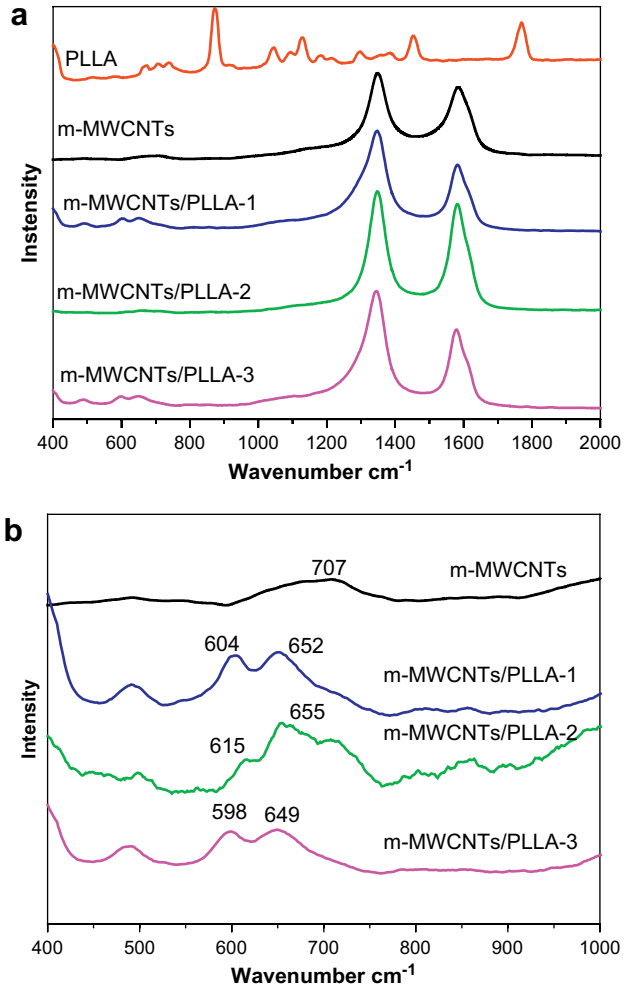

Fig. 4. a) Raman spectra of PLLA, *m*-MWCNTs and *m*-MWCNTs-*g*-PLLA and b) Raman spectra between 400 and 1000 cm^{-1} of *m*-MWCNTs and *m*-MWCNTs-*g*-PLLA.

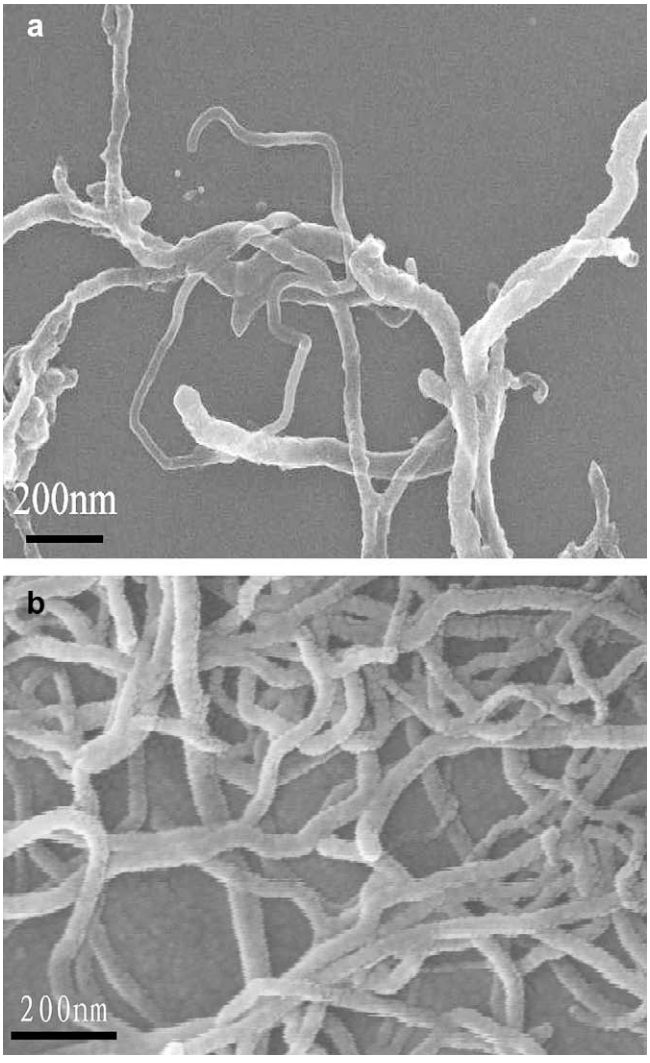

Fig. 5. SEM images of (a) *m*-MWCNTs, (b) *m*-MWCNTs-*g*-PLLA-2.

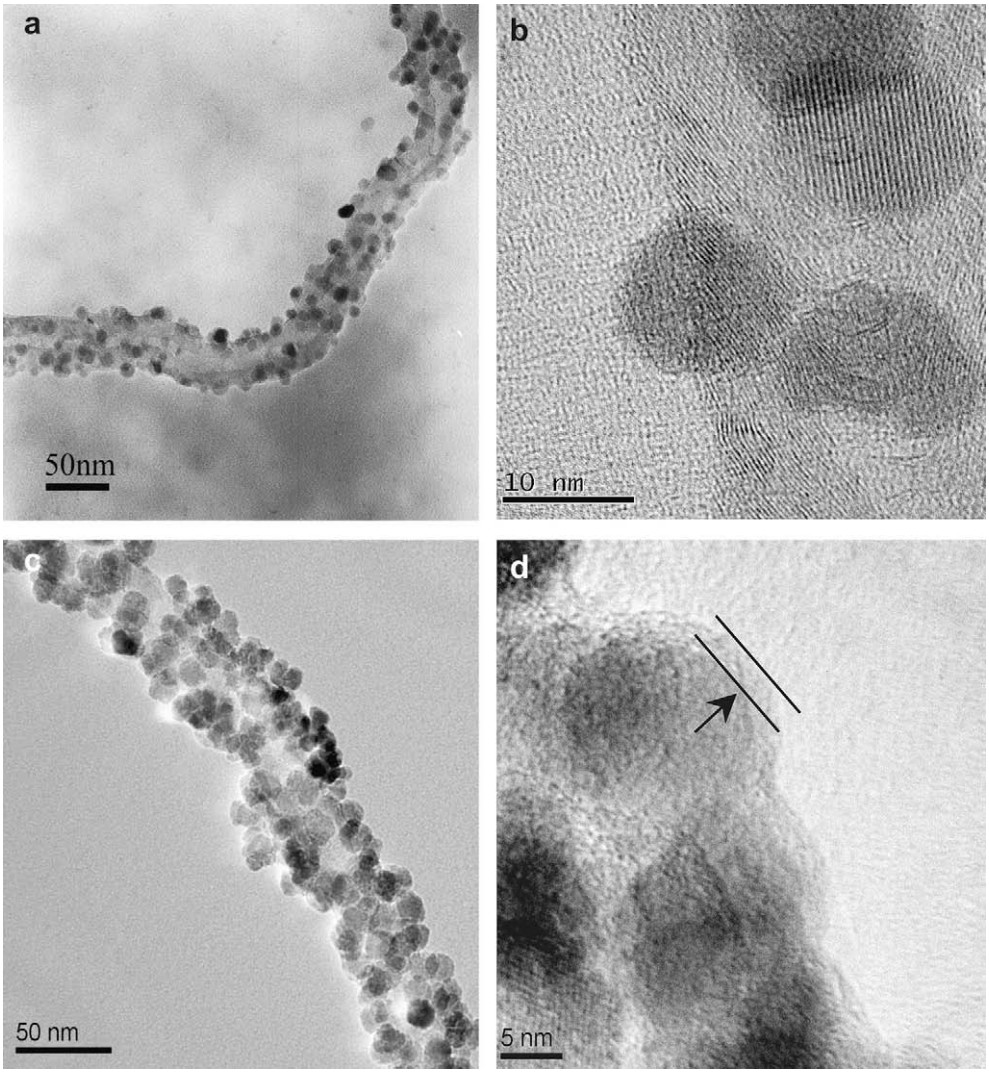

Fig. 6. TEM images of *m*-MWCNTs (a) (b) and *m*-MWCNTs-*g*-PLLA-2 (c) (d).

stretching vibration, respectively. All of the results confirm that PLLA has been grafted onto the sidewalls of *m*-MWCNTs. The large FT-IR band observed at 3445 cm^{-1} are attributed to the asymmetric bending of hydroxyl group bound to the surface of *m*-MWCNTs [16] (Fig. 3b and c), which initiates the polymerization of lactide monomer together with $Sn(Oct)_2$.

The Raman spectra of PLLA, *m*-MWCNTs and *m*-MWCNTs-*g*-PLLA are shown in Fig. 4a. For the *m*-MWCNTs, the D and G bands, attributed to the defects, disorder-induced modes and in-plane E_{2g} zone-center mode [20], are clearly shown at 1349 and 1583 cm^{-1}. There is no shift for the PLLA functionalized *m*-MWCNTs, although D and G bands are also strongly observed. The D^* mode with wavenumber of 2697 cm^{-1} is a second-order overtone mode and is not a disorder-induced mode. Thus, all peaks are normalized against the D^* mode prior to any intensity comparison. The relative intensity and the full width at half maximum intensity (fwhm) of D mode increase markedly upon the formation of the *m*-MWCNTs-*g*-PLLA. However, the G mode of *m*-MWCNTs-*g*-PLLA exhibits a decrease of the fwhm and a small increase in relative intensity (Table 2). The relatively intensity of D mode decreases with increase in the content of PLLA. It seems that the degree of order for *m*-MWCNTs-*g*-PLLA improves, when the grafting PLLA increased. Whereas, G mode exhibits a small decrease in the relative intensity with increase in the content of PLLA. It is inferred that the structural disorder of *m*-MWCNTs is affected by grafting PLLA. It is noteworthy that Raman signals of the grafted PLLA chains are not detected for the *m*-MWCNTs-*g*-PLLA samples; it can be inferred that the PLLA layer on the *m*-MWCNTs is transparent and quite thin. Interestingly, for the *m*-MWCNTs-*g*-PLLA, the peak, ascribed to magnetic particles (bound to *m*-MWCNTs), red-shifts from 707 to 649 cm^{-1} and is divided into two peaks (Fig. 4b). These changes can be possibly attributed to the energy transfer between *m*-MWCNTs and PLLA chains in the process of polymerization. Further studies are needed to fully understand the interactive mechanism between *m*-MWCNTs and PLLA chains.

The typical SEM images of pristine *m*-MWCNTs and *m*-MWCNTs-*g*-PLLA are shown in Fig. 5. Generally, in contrast to the pristine *m*-MWCNTs, the *m*-MWCNTs-*g*-PLLA look thicker and the tubelike nanostructure could still be clearly observed (Fig. 5a and b). As an additional and more direct evidence for the covalent functionalization of PLLA onto *m*-MWCNTs, analysis of TEM is conducted and the typical results are shown in Fig. 6. The average outer diameter of *m*-MWCNTs and *m*-MWCNTs-*g*-PLLA can be estimated to be about 50 ± 5 nm (Fig. 6a and c). At higher magnification, the surface of pristine *m*-MWCNTs seems to be smooth and clear without any extra phase adhering to them (Fig. 6b). However, as shown in Fig 6d, it can be seen that

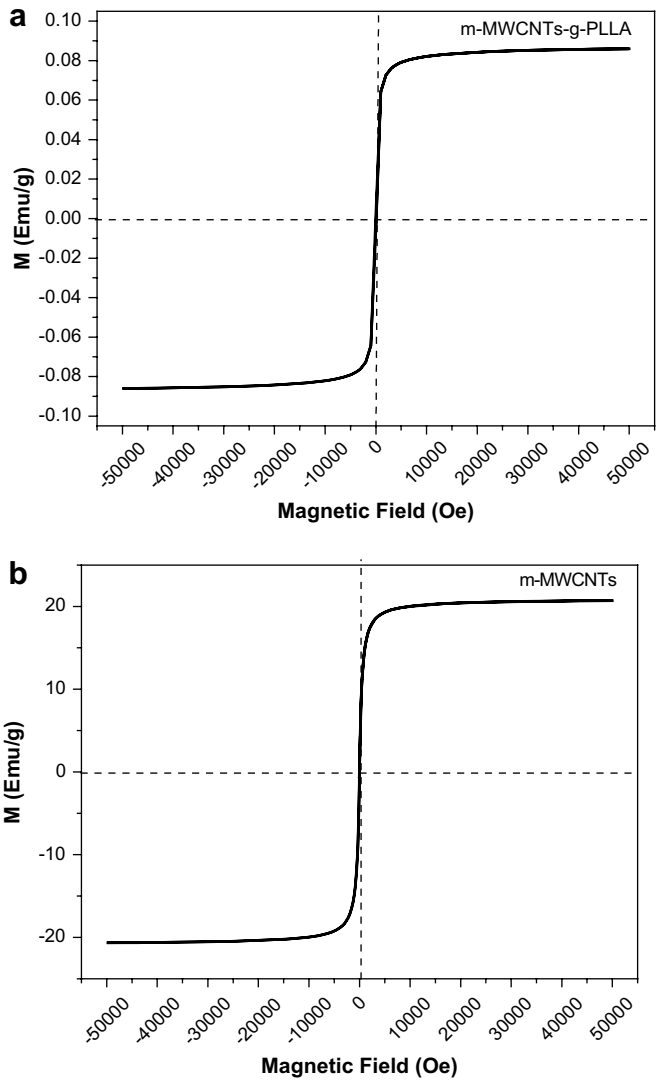

Fig. 7. Magnetization curves of (a) *m*-MWCNTs-*g*-PLLA and (b) *m*-MWCNTs.

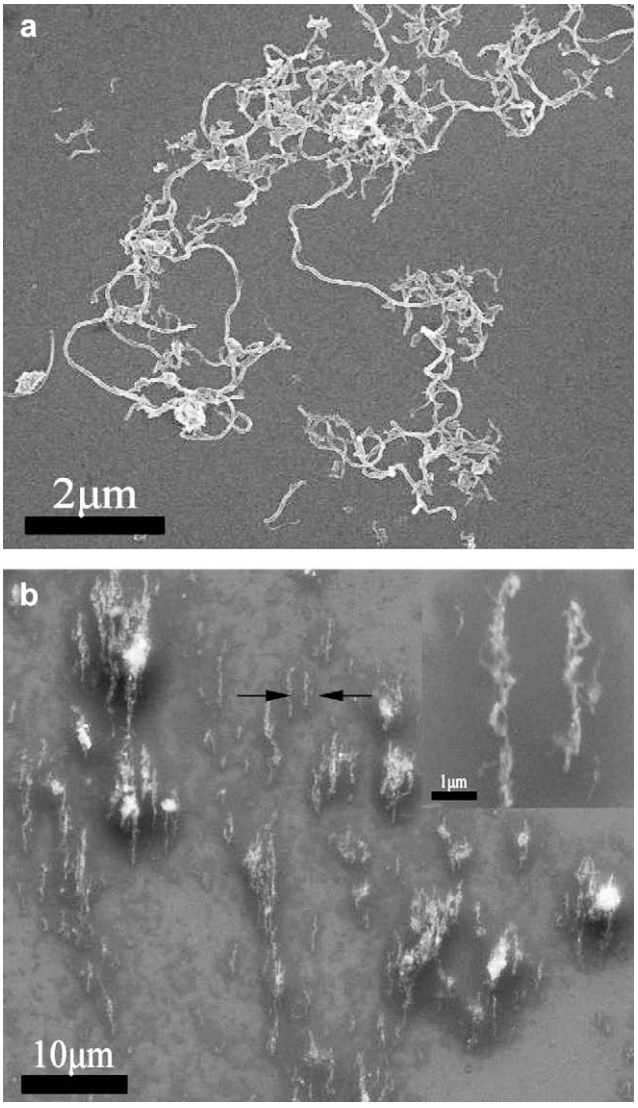

Fig. 9. SEM images of *m*-MWCNTs-*g*-PLLA in the absence (a) and presence (b) of an external magentic field.

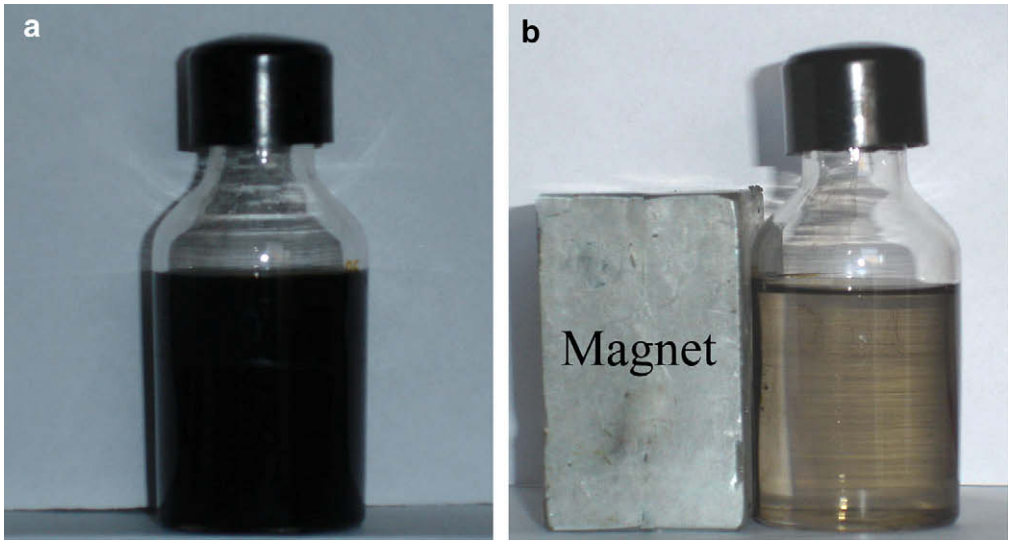

Fig. 8. Photograph of (a) *m*-MWCNTs-*g*-PLLA dispersed in chloroform and (b) their response to a magnet.

amorphous polymer with a thickness of ~2.5 nm covers the surface of *m*-MWCNTs (Fig. 6d), confirming the success of PLLA grafting onto the *m*-MWCNTs surface.

Fig. 7 shows a magnetic hysteresis curve of *m*-MWCNTs-*g*-PLLA and *m*-MWCNTs. Both of them exhibit typical superparamagnetic behavior with no coercivity and remanence. In contrast to *m*-MWCNTs, the saturated magnetization of *m*-MWCNTs-*g*-PLLA decreases due to the diamagnetic grafted PLLA. However, *m*-MWCNTs-*g*-PLLA can be removed controllably by a magnet (Fig. 8). The superparamagnetic performance of *m*-MWCNTs-*g*-PLLA will make it possible to align in PLLA matrix under a low magnetic field.

Fig. 9 shows the behavior of *m*-MWCNTs-*g*-PLLA in the absence and the presence of a 0.1 T magnetic field, when a drop of dispersion of *m*-MWCNTs-*g*-PLLA is dried on the Si wafer. It could be seen that *m*-MWCNTs-*g*-PLLA randomly disperse on the surface of silicon wafer (Fig. 9a), whereas, *m*-MWCNTs-*g*-PLLA can be oriented by applying an external magnetic field (paralleled to the silicon substrate) at 300 K (Fig. 9b). *m*-MWCNTs-*g*-PLLA are aligned by paralleling to the magnetic field and long-chain structure is formed (inserted image in Fig. 9b).

4. Conclusions

PLLA is successfully attached through covalent bonding to *m*-MWCNTs by surface initiated ring-opening polymerization. *m*-MWCNTs-*g*-PLLA remain intact nanostructure after polymerization and the grafted PLLA layer on the *m*-MWCNTs is uniform. Additionally, the amount of the grafted PLLA can be roughly adjusted by the feed ratio of monomer to *m*-MWCNTs. *m*-MWCNTs-*g*-PLLA exhibit typical superparamagnetic performance and can be aligned under lower magnetic field. The results present potential applications for the functional *m*-MWCNTs-*g*-PLLA in biocomposites, drug targeting, tissue engineering and bone regeneration.

Acknowledgment

The authors acknowledge the financial support of the research from the National Basic Research Program of China (No. 2006CB708609) and Hei Longjiang Province Fund for Distinguished Young's Scholars (No. JC200715). They also appreciate Prof. Wang Yinong in Dalian University of Technology for TEM analyzing.

References

[1] Iijima S. Nature 1991;354:56–8.
[2] Wong EW, Sheehan PE, Lierber CM. Science 1997;277:1971–5.
[3] Vivekchand SRC, Sudheendra L, Sandeep M, Govindaraj A, Rao CNR. J Nanosci Nanotechnol 2002;2:631–5.
[4] Ajayan PM, Schadler LS, Giannaris C, Rubio A. Adv Mater 2000;12:750–3.
[5] Kearns JC, Shambaugh RL. J Appl Polym Sci 2002;86:2079–84.
[6] Ikada Yoshito, Tsuji Hideto. Macromol Rapid Commun 2000;21:117–32.
[7] Jain RA. Biomaterials 2000;21:2475–90.
[8] Claes LE. Clin Mater 1992;10:41–6.
[9] Bleach NC, Nazhat SN, Tanner KE, Kellomaki M, Tormala P. Biomaterials 2002;23:1579–85.
[10] Kai Zhang, Yunbing Wang, Hillmyer Marc A, Francis Lorraine F. Biomaterials 2004;25:2489–500.
[11] Guang-Xin Chen, Hun-Sik Kim, Hyun Park Byung, Jin-San Yoon. J Phys Chem B 2005;109:22237–43.
[12] Guang-Xin Chen, Hun-Sik Kim, Hyun Park Byung, Jin-San Yoon. Macromol Chem Phys 2007;208:389–98.
[13] Hun-Sik Kim, Byung Hyun Park, Jin-San Yoon, Hyoung-Joon Jin. Eur Polym J 2007;43:1729–35.
[14] Kimura T, Ago H, Tobita M, Ohshima S, Kyotani M, Yumura M. Adv Mater 2002;14:1380–3.
[15] Kordàs Krisztiàn, Mustonen Tero, Tóth Géza, Vähäkangas Jouko, Uusimäki Antti. Chem Mater 2007;19:787–91.
[16] Wan JQ, Cai W, Feng JT, Liu EZ. J Mater Chem 2007;17:1188–92.
[17] Kricheldorf HR, Kreisersaunders I, Boettcher C. Polymer 1995;36:1253–9.
[18] Kricheldorf HR. Chemosphere 2001;43:49–54.
[19] Kowalski A, Duda A, Penczek S. Macromolecules 2000;33:7359–70.
[20] Jorio A, Pimenta MA, Souza Filho AG, Saito R, Dresselhaus G, Dresselhaus MS. New J Phys 2003;139:1–17.